JOURNAL OF CHEMICAL & ENGINEERING DATA

ARTICLE

pubs.acs.org/jced

Adsorption of Silver(I) from Aqueous Solution by Chelating Resins with 3-Aminopyridine and Hydrophilic Spacer Arms: Equilibrium, Kinetic, Thermodynamic, and Mechanism Studies

Shuhui Song, Chunnuan Ji,* Min Wang, Chunrong Wang, Changmei Sun, Rongjun Qu, Chunhua Wang, and Hou Chen

School of Chemistry and Materials Science, Ludong University, Yantai 264025, China

ABSTRACT: The equilibrium, kinetics, thermodynamics, and mechanism of two novel chelating resins with 3-aminopyridine and hydrophilic spacer arms (denoted as PS-DEG-3-AP and PS-TEG-3-AP) for Ag(I) were investigated in detail. The Boyd, Langmuir, Freundlich, and Dubinin−Radushkevich (D-R) models were applied to describe the adsorption of the resins for Ag(I). The saturated adsorption capacities of PS-DEG-3-AP and PS-TEG-3-AP for Ag(I) were (0.21 and 0.30) mmol·g^{-1} at pH 4, respectively. The results showed that the adsorption processes were governed by film diffusion and followed the pseudo second-order model well. The Langmuir model was better than the Freundlich model to describe the isotherm process. The *E* values obtained from the D−R model indicated that the adsorption of Ag(I) ions onto the resins occurred by chemical ion exchange. The adsorption mechanism of the resins for Ag(I) was confirmed by X-ray photoelectron spectroscopy (XPS). The XPS results clarified that not only 3-aminopyridine but also S atoms existed in the spacer arm that could take part in the coordination with Ag(I). Five adsorption−desorption cycles were conducted for the reuse of the resins. The results indicated that these two resins were suitable for reuse without considerable change in adsorption capacity.

1. INTRODUCTION

Silver is widely used in medicine, the disinfection of water, photography, electronic devices, mirrors, alloys, cloud seeding, and jewelry owing to its resistance to corrosion and marked antibacterial properties. Recently, the increasing use of silver and silver compounds has resulted in an increased silver content in environmental samples.[1−3] Silver can also enter into the environment via industrial water because it often occurs as an impurity in copper, zinc, arsenic, and antimony industries, and silver has been recognized as a toxic element to microorganisms or larval forms of aquatic animals.[4] Silver also might pose a potential risk as a water pollutant because of the lack of recycling of mined silver.[5] Thus, the removal and recovery of silver from wastewater is very critical. Numerous processes include chemical precipitation, ion exchange, and solvent extraction; biosorption and adsorption have been used for the removal of heavy metal ions from aqueous solution.[6−9] Among these, adsorption using chelating resins is found to be one of the most efficient methods for the removal and recovery of silver.[10−13]

In general, the adsorption selectivity of chelating resins has been reported to be dependent mainly on the chelate forming properties of functional groups chemically bonded on supports such as silica gel, cellulose, and macroporous copolymers. Thus, the functional groups play an important role in the adsorption capacity, effectiveness, and selectivity of the chelating resins.[14−16] Recently, it has been proved that chelating resins containing heterocyclic functional groups such as pyridine, imidazole, thiazole, and so forth possess excellent adsorption and selectivity properties for metal ions, especially for noble metal ions.[17−20] Among the above-mentioned heterocyclic functional groups, aminopyridine is one of the common functional groups used to prepare chelating resins.[21,22]

When chelating resins are used in aqueous solutions to remove and recover metal ions, hydrophilic resins are preferred to hydrophobic systems. Often, the hydrophobicity of the resin make it difficult for metal ions to swell in water and to diffuse into the interior of chelating resins, which limits the coordination of functional groups with metal ions.[23] To overcome this problem, many attempts have been made to improve the hydrophilicity of chelating resins by introducing hydrophilic spacer arms between the functional group and the polymeric matrix. It has been demonstrated that the introduction of the hydrophilic spacer arms can enhance the hydrophilicity of the polymeric ligands and increase the adsorption capacity and the adsorption rate of the chelating resins.[24−26]

In our previous paper,[27] two novel chelating resins containing 3-aminopyridine and hydrophilic spacer arms of ethylene oxide and ethylene sulfide, which were denoted as PS-DEG-3-AP and PS-TEG-3-AP (see Scheme 1), were synthesized and characterized. Our preliminary experimental results showed that the resins exhibited higher affinities for Hg(II) and Ag(I). As subsequent work, the objective of the present work is to investigate the adsorption equilibrium, kinetics, thermodynamics, and mechanism of the resins for Ag(I) in aqueous solution. The regeneration of the resins for Ag(I) was also investigated.

2. EXPERIMENTAL SECTION

2.1. Materials. PS-DEG-3-AP and PS-TEG-3-AP were used as materials (see Scheme 1). Their synthesis and characterization were reported in our previous work.[27] All chemical reagents used

Special Issue: John M. Prausnitz Festschrift

Received: October 6, 2010
Accepted: March 1, 2011
Published: March 11, 2011

Scheme 1. Structure of PS-DEG-3-AP and PS-TEG-3-AP

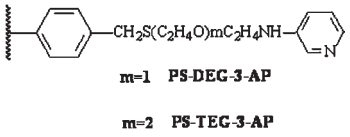

in this study were of analytical grade and used without further purification. The Ag(I) stock solution (0.1 mol·L^{-1}) was prepared by dissolving appropriate amounts of analytical grade nitrate in distilled water and further diluted prior to use. Buffer solutions of pH 1.0 to 6.0 were prepared by addition of dilute nitric acid or liquid ammonia to 0.1 mol·L^{-1} ammonium acetate solution.

2.2. Instruments. A pH meter (Mettler-Toledo, LE438 pH, China) was used for the measurement of pH values. The concentrations of metal ions were measured on a GBC-932 atomic absorption spectrophotometer (AAS) (Victoria, Australia), equipped with an air-acetylene flame. X-ray photoelectron spectroscopy (XPS) spectra were collected on a PHI 1600ESCA system (Perkin-Elmer Co.). Test conditions were as follows: Mg Kα (1253.6 eV), power 200.0 W, resolution 187.85 Ev.

2.3. Adsorption Procedures. *2.3.1. Effect of pH on Adsorption.* Adsorption capacities of the resins at different pH values were determined by batch tests according to the typical procedure: 30 mg of the resin was added to a mixture of 19 mL of a 0.1 M ammonium acetate buffer solution at definite pH values and 1 mL of a 0.1 M aqueous solution of Ag(I) in a 100 mL glass bottle with a stopper. After being shaken at 298 K for 24 h, the solution was separated from the resin. The concentration of metal ions in the solution was determined by the AAS. The adsorption capacity was calculated according to eq 1.

$$Q = \frac{(C_0 - C)V}{W} \quad (1)$$

where Q is the adsorption capacity (mmol·g^{-1}); C_0 and C are the initial concentration and the concentration at any time t, respectively, of metal ion in solution (mmol·mL^{-1}); V is the solution volume (mL); and W is the dry weight of resins (g). Each determination in the adsorption procedure was repeated three times, and the results are given as average values. Error bars are also indicated wherever necessary.

2.3.2. Adsorption Kinetics. To obtain the data of adsorption kinetics, 30 mg of the resin was added to 20.0 mL of 0.005 mol·L^{-1} metal ion solution (pH 4.0). The mixture was shaken continuously in a thermostat-cum-shaking assembly at a predetermined temperature. Aliquots of 1 mL solution were withdrawn at predetermined intervals, and the concentration of Ag(I) in the solution was determined by the AAS. The amount of Ag(I) sorbed on the resin was calculated from the difference between amounts of Ag(I) in the solution and the starting solution according to eq 1.

2.3.3. Adsorption Isotherms. The isothermal adsorption was also investigated by batch tests. A typical procedure was as follows: a series of 100 mL test tubes were employed. Each test tube was filled with 30 mg of the resin and 20 mL of Ag(I) of varying concentrations and adjusted to pH 4 and the desired temperature. After a shaking time of 24 h, the solution was separated from the adsorbent, and the residual concentration of Ag(I) was also determined by the AAS. The adsorption capacities were calculated also according to eq 1, where C is the equilibrium concentration of Ag(I) in solution.

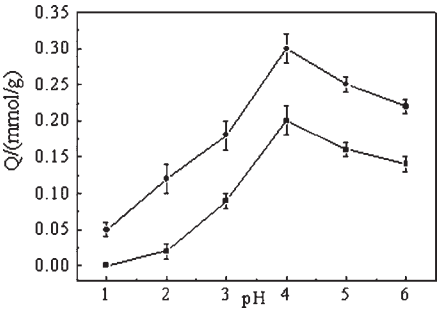

Figure 1. Effect of pH on the adsorption of PS-DEG-3-AP (-■-) and PS-TEG-3-AP (-●-) for Ag(I) (conc. of Ag(I): 0.005 mol·L^{-1}, pH 4.0, resin: 30 mg).

2.3.4. Regeneration of the Resins. To assess the reusability of PS-DEG-3-AP and PS-TEG-3-AP, consecutive adsorption−desorption cycles were repeated five times using the same resin. A solution of 3 % thiourea in 0.1 mol·L^{-1} HNO_3 was employed as the desorption agent. The Ag(I)-loaded PS-DEG-3-AP or PS-TEG-3-AP was placed in this medium, and then the mixtures were shaken for 60 min at room temperature (primary experiments indicated that Ag(I) adsorbed on the resin was almost desorbed completely when the contact time of Ag(I)-loaded PS-DEG-3-AP or PS-TEG-3-AP with this medium was about 40 min). The final concentration of Ag(I) in the aqueous phase was determined by the AAS. After determination of the metal content, the resin was washed with excess of the base solution and distilled water to reuse for the next experiment.

3. RESULTS AND DISCUSSION

3.1. Effect of pH on Adsorption. The pH value is a critical parameter in the adsorption process. It not only affects the electronic status of the functional groups but may also alter the speciation of the metal ions in the solution.[28] The effect of pH on the adsorption of the resins for Ag(I) was investigated within the pH range of 1 to 6 at 298 K. Figure 1 shows the changes of Ag(I) adsorption on the resins with varying pH values. With pH 1 to 4, the adsorption capacities increased with the increase of the pH value in the solution. This is probably because the N atoms in 3-aminopyridine could easily be protonized at lower pH conditions and thus lose coordination ability. Also, the experiments showed that at higher pH conditions (> 4), the adsorption capacities decreased with the increasing pH value. Similar experimental phenomena have also been reported in the literature.[1,11] The problem arises in part from the coordination bonding resulting from the S atom present in the spacer arms. It is understandable that the concentration of nitrate ion decreases with the increase of pH. Because of the existence of the equilibrium equation among Ag(I), the S atom, and nitrate ion, the adsorption capacities of the resins for Ag(I) decrease with decreasing concentration of NO_3^- in the metallic solution.[29] On the other hand, the maximum adsorption capacities of PS-DEG-3-AP and PS-TEG-3-AP for Ag(I) were (0.20 and 0.30) mmol·g^{-1}, respectively. According to these results, the pH in the solution would be kept at 4.0 in subsequent experiments. In addition, one could note that the adsorption capacity of PS-TEG-3-AP for Ag(I) was higher than that of PS-DEG-3-AP, which meant that the adsorption capacity increased with the increase of the length of the spacer arm. A reasonable explanation for this was that the increase of spacer arm might increase both the flexibility of the functional group and the hydrophilicity, which would be beneficial for the functional group to coordinate with the metal ion.[23]

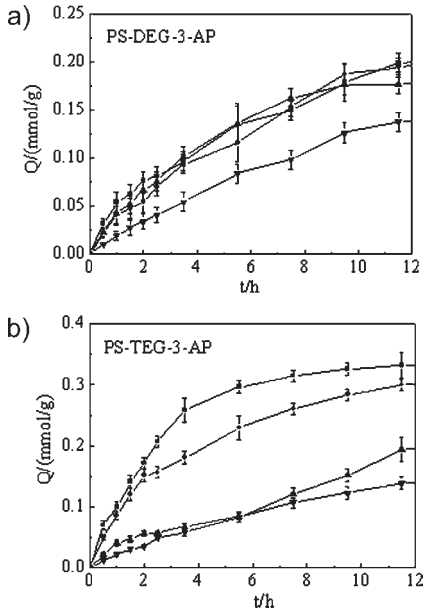

Figure 2. Adsorption capacities of Ag(I) versus time on PS-DEG-3-AP and PS-TEG-3-AP at different temperatures (conc. of Ag(I): 0.005 mol·L^{-1}; pH 4.0; resin: 30 mg; temperatures: -■-, 308 K; -●-, 298 K; -▲-, 288 K; -▼-, 278 K).

3.2. Adsorption Kinetics. Figure 2 shows the adsorption kinetics of PS-DEG-3-AP and PS-TEG-3-AP for Ag(I) at different temperatures. From Figure 2, it can be noted that the adsorption equilibrium of PS-DEG-3-AP and PS-TEG-3-AP for Ag(I) was obtained in 12 h. So the contact period was selected as 12 h in all equilibrium tests. The temperature of solution affected the adsorption capacities significantly, that was, the adsorption capacities increased with the increasing of temperature. The reason for this could be ascribed to the through swelling of the resins at higher temperature, which made it easier for Ag(I) to diffuse into the interior of the resins more easily.

The Boyd et al.[30] and Reichenberg[31] equations were applied to the experimental data to clarify the adsorption kinetics of Ag(I) on the resins. The data in Figure 2 were analyzed by the following equations:

$$F = 1 - \frac{6}{\pi^2} \sum_{n-1}^{\infty} \frac{1}{n^2} \left[\frac{-D_i t \pi^2 n^2}{{r_0}^2} \right] \quad (2)$$

or

$$F = 1 - \frac{6}{\pi^2} \sum_{n-1}^{\infty} \frac{1}{n^2} \exp[-n^2 Bt] \quad (3)$$

where F is the fractional attainment of equilibrium at time t and is obtained by the expression

$$F = \frac{Q_t}{Q_0} \quad (4)$$

where Q_t is the amount of adsorbate taken up at time t and Q_0 is the maximum equilibrium uptake and

$$B = \frac{\pi^2 D_i}{{r_0}^2} = \text{time constant} \quad (5)$$

where D_i is the effective diffusion coefficient of the ion in the adsorbent phase; r_0 is the radius of the adsorbent particle, assumed to be spherical; and n is an integer that defines the infinite series solution.

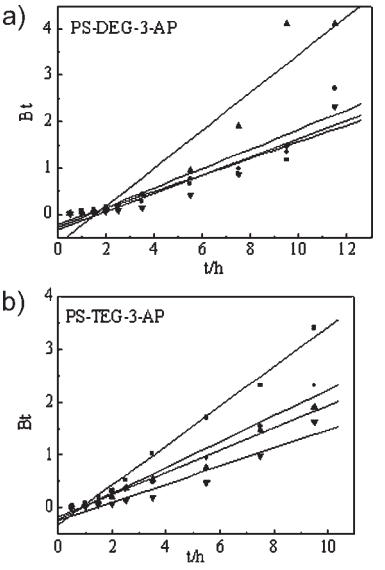

Figure 3. B_t vs time plots at different temperatures of PS-DEG-3-AP and PS-TEG-3-AP for Ag(I) (temperatures: -■-, 308 K; -●-, 298 K; -▲-, 288 K; -▼-, 278 K).

Table 1. B_t versus Time Linear Equations and Coefficients R^2 and Intercept Errors

resin	T/K	linear equation	R^2	intercept errors
PS-DEG-3-AP	308	$B_t = 0.1787t - 0.2228$	0.9007	0.0209
	298	$B_t = 0.2105t - 0.2781$	0.9008	0.0247
	288	$B_t = 0.4098t - 0.6448$	0.9202	0.0427
	278	$B_t = 0.1962t - 0.3424$	0.9150	0.0216
PS-TEG-3-AP	308	$B_t = 0.3749t - 0.3243$	0.9895	0.0146
	298	$B_t = 0.2458t - 0.2255$	0.9725	0.0156
	288	$B_t = 0.2116t - 0.1796$	0.9811	0.0111
	278	$B_t = 0.1724t - 0.2472$	0.9301	0.0179

B_t values were obtained for each observed value of F from Reichenberg's table,[31] and the results are plotted in Figure 3. The adsorption procedure of adsorbents for metal ions is considered to take place through two mechanisms of film diffusion and particle diffusion. The linearity test of B_t versus time plots was employed to distinguish between film diffusion and particle diffusion controlled adsorption. If the plot was a straight line passing through the origin, the adsorption process should be dominated by the particle diffusion mechanism, or else it might be governed by film diffusion. The linear equations and coefficients of determination (R^2) are given in Table 1. Figure 3 shows that the four straight lines for each resin under different temperatures did not pass through the origin, indicating that the rate-controlling step is not particle diffusion, but film diffusion.

The adsorption kinetics data of Ag(I) on the resins were also performed by pseudo first-order and pseudo second-order models given below as eqs 6 and 7, respectively.

$$\log(Q_0 - Q) = \log Q_0 - \frac{k_1}{2.303} t \quad (6)$$

$$\frac{t}{Q} = \frac{1}{k_2 {Q_0}^2} + \frac{1}{Q_0} t \quad (7)$$

where k_1 is the rate constant of pseudo first-order adsorption (h^{-1}); k_2 is the rate constant of pseudo second-order adsorption

dx.doi.org/10.1021/je101002b |J. Chem. Eng. Data 2011, 56, 1001–1008

($g \cdot mmol^{-1} \cdot h^{-1}$); Q_0 and Q are the adsorption amounts at equilibrium and at time t, respectively ($mmol \cdot g^{-1}$).

Both of the models were used to fit the kinetics curves, and the results showed that the pseudo second-order model was more suitable since the values of R^2 could be regarded as a measure of the goodness-of-fit of experimental data on the kinetic models.[32] The straight lines of the pseudo second-order kinetic model are shown in Figure 4. The corresponding parameters calculated according to the models are tabulated in Table 2.

From Table 2, two conclusions could be obtained: (1) The values of k_2 of PS-TEG-3-AP for Ag(I) at the four temperatures were higher than those of PS-DEG-3-AP. The results might ascribe to the increase of ethylene oxide groups in the spacer arms, which could increase the hydrophilicity, and then enhance the adsorption rates. (2) For the same kind of resin, the values of k_2 of the resin for Ag(I) increased with an increase of temperature. This meant that the adsorption of PS-DEG-3-AP and PS-TEG-3-AP for Ag(I) was an endothermic process and high temperature was of benefit to the adsorption. These conclusions are concordant with the results presented in Figure 2.

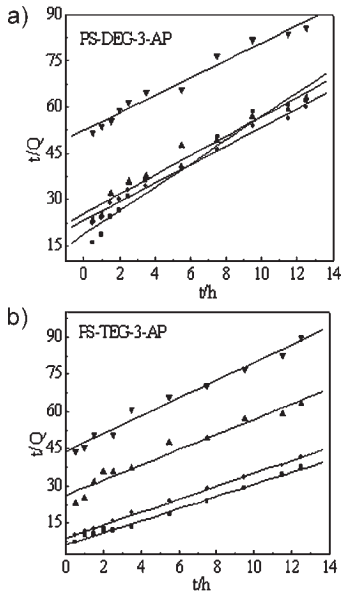

Figure 4. Pseudo second-order kinetic model of PS-DEG-3-AP and PS-TEG-3-AP for Ag(I) (temperatures: -■-, 308 K; -●-, 298 K; -▲-, 288 K; -▼-, 278 K).

According to the Arrhenius equation:

$$\ln k_2 = -E_a/RT + \ln A \tag{8}$$

where k_2 is the constant of adsorption obtained from pseudo second-order rate equations, A is the pre-exponential factor, R is the gas constant, T is the temperature, and E_a is the apparent activation energy of adsorption. Two straight lines were obtained by plotting $\ln k_2$ against $1/T$ (see Figure 5). The apparent activation energies of adsorption E_a calculated from the linear slopes were (36.50 and 29.34) $kJ \cdot mol^{-1}$ for PS-DEG-3-AP and PS-TEG-3-AP, respectively. These low activation energies as compared to these of typical chemical reactions of (65 to 250) $kJ \cdot mol^{-1}$ indicate that the adsorption of PS-DEG-3-AP and PS-TEG-3-AP for Ag(I) was a facile procedure.

3.3. Adsorption Isotherms. The adsorption isotherms of PS-DEG-3-AP and PS-TEG-3-AP for Ag(I) were investigated at four different temperatures, and the data were analyzed with the Langmuir (eq 9) and Freundlich (eq 10) equations, respectively. Then, Figure 6 was obtained.

$$\frac{C}{Q} = \frac{1}{bQ_0} + \frac{C}{Q_0} \tag{9}$$

$$\ln Q = \ln K_F + \frac{1}{n} \ln C \tag{10}$$

where Q is the adsorption capacity ($mmol \cdot g^{-1}$), C is the equilibrium concentration of metal ions ($mol \cdot L^{-1}$), Q_0 is the saturated adsorption capacity ($mmol \cdot g^{-1}$), b is an empirical parameter, n is the Freundlich constant, and K_F is the binding

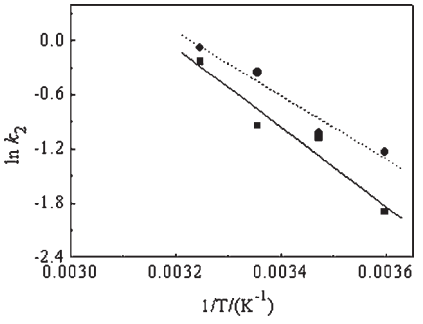

Figure 5. $\ln k_2$ vs $1/T$ plots for the adsorption of PS-DEG-3-AP (-■-) and PS-TEG-3-AP (-●-) for Ag(I).

Table 2. Kinetic Parameters of PS-DEG-3-AP and PS-TEG-3-AP for Ag(I) at Different Temperatures

		pseudo first-order model			pseudo second-order model		
resin	T/K	k_1 (h^{-1})	Q_0 ($mmol \cdot g^{-1}$)	R^2	k_2 ($g \cdot mmol^{-1} \cdot h^{-1}$)	Q_0 ($mmol \cdot g^{-1}$)	R^2
PS-DEG-3-AP	308	0.21	0.20	0.9346	0.79	0.26	0.9632
	298	0.29	0.26	0.8756	0.39	0.33	0.9839
	288	0.28	0.27	0.8727	0.34	0.31	0.9609
	278	0.21	0.17	0.9216	0.15	0.35	0.9694
PS-TEG-3-AP	308	0.45	0.39	0.9779	0.92	0.41	0.9933
	298	0.47	0.48	0.8027	0.70	0.43	0.9924
	288	0.24	0.26	0.6870	0.36	0.32	0.9546
	278	0.27	0.42	0.7430	0.29	0.28	0.9821

dx.doi.org/10.1021/je101002b |J. Chem. Eng. Data 2011, 56, 1001–1008

energy constant reflecting the affinity of the resin onto metal ions.

As is well-known, the basic assumption of the Langmuir theory is that the adsorption takes place at specific homogeneous sites within the adsorbent. On the other hand, the Freundlich model assumes that the adsorption occurs on a heterogeneous surface.[33] The parameters for the two isotherms obtained from experimental data were presented in Table 3. The coefficients of determination (R^2) fitted with the Langmuir model were higher than those obtained from the Freundlich model, indicating that the adsorption of Ag(I) on PS-DEG-3-AP and PS-TEG-3-AP fitted better the Langmuir model.

The Dubinin−Radushkevich (D-R) isotherm model was also applied to the equilibrium data to determine the nature of adsorption processes as physical or chemical.[34] The linear presentation of the D-R isotherm equation[35] is expressed by

$$\ln Q_e = \ln Q_m - \beta\varepsilon^2 \qquad (11)$$

where Q_e is the amount of metal ions adsorbed on per unit weight of resin ($\mathrm{mol\cdot g^{-1}}$), Q_m is the maximum adsorption capacity ($\mathrm{mol\cdot g^{-1}}$), β is the activity coefficient related to the adsorption mean free energy ($\mathrm{mol^2\cdot J^{-2}}$), and ε is the Polanyi potential ($\varepsilon = RT\ln(1 + 1/C_e)$).

The mean free energy (E; $\mathrm{kJ\cdot mol^{-1}}$) is calculated by using the β value:

$$E = \frac{1}{\sqrt{2\beta}} \qquad (12)$$

The E value gives information about the adsorption mechanism, physical or chemical. If it lies between (8 and 16) $\mathrm{kJ\cdot mol^{-1}}$, the adsorption process takes place chemically, while at $E <$ 8 $\mathrm{kJ\cdot mol^{-1}}$, the adsorption process proceeds physically. Figure 7 and Table 4 show the results and the corresponding parameters in the D-R model of the resins for Ag(I). The E values of PS-DEG-3-AP and PS-TEG-3-AP for Ag(I) at the four temperatures were in the range of (8.34 to 10.01) $\mathrm{kJ\cdot mol^{-1}}$. These results implied that the adsorption processes of Ag(I) onto PS-DEG-3-AP and PS-TEG-3-AP might proceed by a chemical ion-exchange mechanism.

3.4. Adsorption Mechanism of Resins for Ag(I). On the basis of the above-mentioned conclusion, XPS was employed to

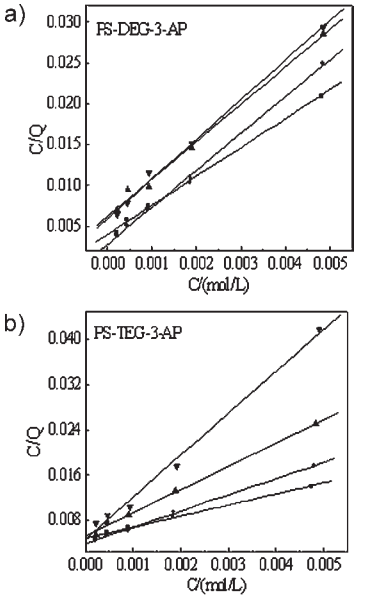

Figure 6. Langmuir isotherms of PS-DEG-3-AP and PS-TEG-3-AP for Ag(I) (temperatures: -■-, 308 K; -●-, 298 K; -▲-, 288 K; -▼-, 278 K).

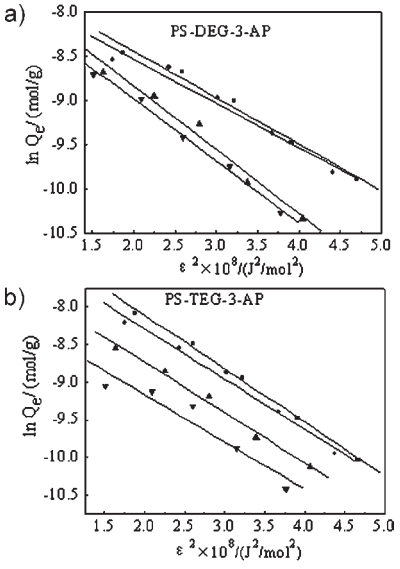

Figure 7. D-R isotherms of PS-DEG-3-AP and PS-TEG-3-AP for Ag(I) (temperatures: -■-, 308 K; -●-, 298 K; -▲-, 288 K; -▼-, 278 K).

Table 3. Parameters in the Langmuir and Freundlich Equations of PS-DEG-3-AP and PS-TEG-3-AP for Ag(I)

		Langmuir parameters			Freundlich parameters		
resin	T / K	Q_0 / ($\mathrm{mmol\cdot g^{-1}}$)	b / ($\cdot 10^{-3}$)	R_L^2	n	K_F	R_F^2
PS-DEG-3-AP	308	0.28	8.7874	0.9969	2.01	3.5717	0.9804
	298	0.22	15.997	0.9970	2.40	2.1106	0.9302
	288	0.22	7.3692	0.9940	1.78	3.8979	0.9557
	278	0.21	8.1694	0.9949	1.97	2.7164	0.9786
PS-TEG-3-AP	308	0.51	3.9890	0.9929	1.50	12.834	0.9919
	298	0.35	7.2473	0.9991	1.78	6.1944	0.9667
	288	0.24	7.8963	0.9963	1.91	3.4843	0.9750
	278	0.13	15.6138	0.9928	2.22	1.6056	0.8717

dx.doi.org/10.1021/je101002b |J. Chem. Eng. Data 2011, 56, 1001–1008

Table 4. Parameters in the D-R Model of PS-DEG-3-AP and PS-TEG-3-AP for Ag(I)

resin	T/K	linear equation	R^2	Q_m ($mmol \cdot g^{-1}$)	E ($kJ \cdot mol^{-1}$)
PS-DEG-3-AP	308	$y = -5.26 \cdot 10^{-9}x - 7.39$	0.9837	0.62	9.75
	298	$y = -4.99 \cdot 10^{-9}x - 7.54$	0.9601	0.53	10.01
	288	$y = -7.19 \cdot 10^{-9}x - 7.40$	0.9753	0.61	8.34
	278	$y = -6.96 \cdot 10^{-9}x - 7.60$	0.9919	0.50	8.48
PS-TEG-3-AP	308	$y = -7.10 \cdot 10^{-9}x - 6.69$	0.9960	1.24	8.39
	298	$y = -6.69 \cdot 10^{-9}x - 6.95$	0.9866	0.96	8.65
	288	$y = -6.67 \cdot 10^{-9}x - 7.40$	0.9883	0.61	8.66
	278	$y = -6.30 \cdot 10^{-9}x - 7.90$	0.9130	0.37	8.91

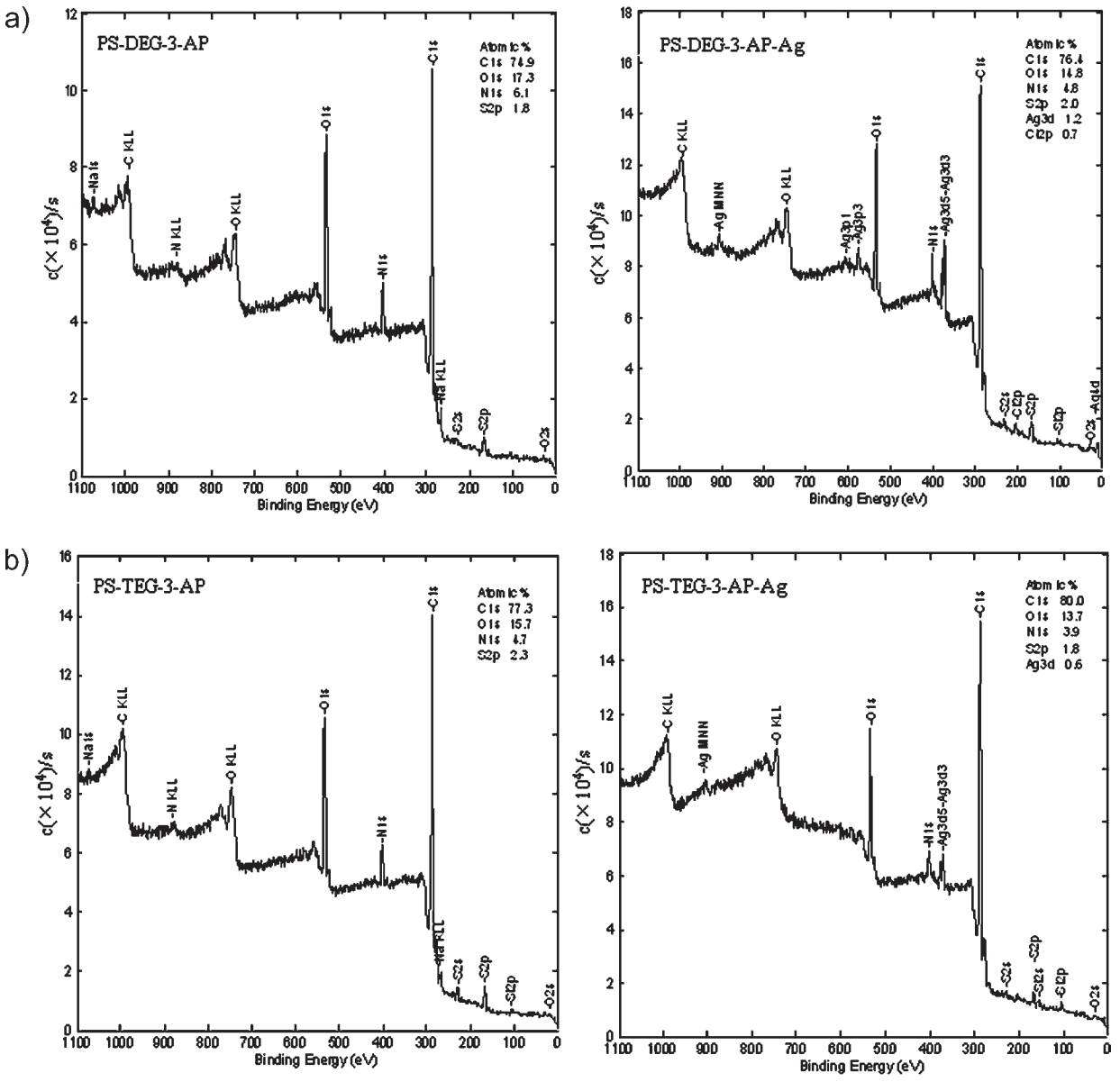

Figure 8. XPS spectra of PS-DEG-3-AP and PS-TEG-3-AP before and after adsorption for Ag(I).

confirm the adsorption mechanism of PS-DEG-3-AP and PS-TEG-3-AP for Ag(I) (see Figure 8).[36] Table 5 shows the XPS data of the resins before and after adsorption of Ag(I). It can seen that the N_{1s} binding energies of PS-DEG-3-AP and PS-TEG-3-AP increased from (399.85 to 401.13 and 399.96 to 401.18) eV, respectively, after the adsorption of Ag(I), meaning that N was an electron donor. The binding energies of S_{2p} in the resins of PS-DEG-3-AP and PS-TEG-3-AP increased by (0.35 and 0.70) eV, respectively, after adsorption, showing that S atoms existed in the spacer arms were also involved in coordinating with Ag(I).

Table 5. Binding Energy (eV) of the Adsorption of PS-DEG-3-AP and PS-TEG-3-AP for Ag(I)

	C_{1s}	N_{1s}	O_{1s}	S_{2p}	Ag_{3d}
PS-DEG-3-AP	284.72	399.85	531.72	167.85	
	286.34		533.26		
	288.22				
PS-DEG-3-AP-Ag	284.75	399.78	531.91	168.20	368.04
	286.24	401.13	533.42		
	288.09				
PS-TEG-3-AP	284.72	399.96	531.83	167.56	
	286.24		533.43		
	288.09				
PS-TEG-3-AP-Ag	284.77	399.97	531.93	168.26	368.93
	286.30	401.18	533.60		
	288.30				
Ag(I)					375.01[35]

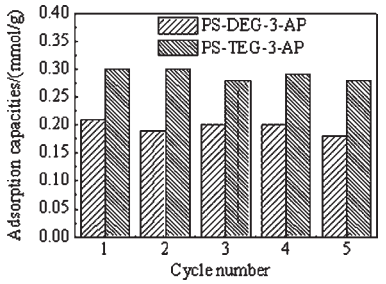

Figure 9. Reusability of PS-DEG-3-AP and PS-TEG-3-AP with the repeated sorption−desorption cycle (conc. of Ag(I): 0.005 mol·L^{-1}, pH 4.0, resin: 30 mg).

Meanwhile, the decreasing values of the binding energies of Ag_{3d} after the adsorption for PS-DEG-3-AP and PS-TEG-3-AP were (6.97 and 6.08) eV, respectively, indicating that Ag atoms were an electron acceptor. From the XPS results it also could be seen that there were little changes in the O_{1s} binding energies of PS-DEG-3-AP and PS-TEG-3-AP after the adsorption of Ag(I). This meant that O atoms did not take part in the coordination with Ag(I) and the existence of it in spacer arms only increased the hydrophilicity of PS-DEG-3-AP and PS-TEG-3-AP.

3.5. Regeneration and Desorption Efficiency. The regeneration of the adsorbent is one of the key factors in assessing its potential for commercial applications. Four kinds of desorption agents such as 0.5 mol·L^{-1} HNO_3, 1 % thiourea in 0.5 mol·L^{-1} HNO_3, 3 % thiourea in 0.5 mol·L^{-1} HNO_3, and 3 % thiourea were chosen as eluents in the desorption of Ag(I) adsorbed in the resins. The 3 % thiourea in 0.5 mol·L^{-1} HNO_3 solution was selected as the desorption agent for Ag(I) due to attaining the best regeneration using this solution. The adsorption capacities of the five adsorption−desorption cycles are shown in Figure 9. The adsorption capacities had a slight decrease after five consecutive adsorption−desorption cycles. This might be due to the ignorable partial plug of pore canals during the adsorption−desorption process. These results indicated that the resins were suitable for repeated use without considerable change in adsorption capacity.

4. CONCLUSIONS

This study focused on the adsorption of Ag(I) from aqueous solution using two novel chelating resins with 3-aminopyridine and hydrophilic spacer arms. The adsorption capacities of PS-DEG-3-AP and PS-TEG-3-AP were (0.21 and 0.30) mmol·g^{-1} at pH 4, respectively. The kinetic data indicated that the adsorption processes were governed by film diffusion and followed the pseudo second-order model well. The Langmuir model was better than the Freundlich model to describe the isotherm process. The *E* values obtained from the D-R model indicated that the adsorption of Ag(I) onto the resins took place by chemical ion exchange. The XPS results suggested that not only 3-aminopyridine but also S atoms existed in the spacer arms could take part in the coordination with Ag(I). The resins could be regenerated by 3 % thiourea in 0.1 M HNO_3 with higher effectiveness. Five adsorption−desorption cycles demonstrated that the resins could be used repeatedly without considerable change in adsorption capacity.

AUTHOR INFORMATION

Corresponding Author

*Tel.: +86 535 6672176; fax: +86 535 6697667. E-mail address: jichunnuan@126.com.

Funding Sources

The authors are grateful for the financial support by the Nature Science Foundation of Shandong Province (Nos. Y2007B19, 2008BS04011) and the Nature Science Foundation of Ludong University (No. LY20072902).

REFERENCES

(1) Dadfarnia, S.; Haji Shabani, A. M.; Gohari, M. Trace enrichment and determination of silver by immobilized DDTC microcolumn and flow injection atomic absorption spectrometry. *Talanta* **2004**, *64*, 682–687.

(2) Shabazi, Z.; Dadfarnia, S.; Shabani, A. M. H.; Jafari, A. A. A sensitive and simple flotation-spectrophotometric method for the determination of microgram amounts of silver using schiff base 2-[(2-mercaptophenylimino)methyl]phenol. *J. Anal. Chem.* **2008**, *63*, 446–450.

(3) Raoof, J. B.; Ojani, R.; Alinezhad, A.; Rezaie, S. Z. Differential pulse anodic stripping voltammetry of silver(I) using *p*-isopropylcalix[6]arene modified carbon paste electrode. *Monatsh. Chem.* **2010**, *141*, 279–284.

(4) Absalan, G.; Akhond, M.; Ghanizadeh, A. Z.; Abedi, Z. A.; Tamami, B. Benzil derivative of polyacrylohydrazide as a new sorbent for separation, preconcentration and measurement of silver(I) ion. *Sep. Purif. Technol.* **2007**, *56*, 231–236.

(5) Noroozifa, M.; Motlagh, M. K.; Taheri, A.; Dorabei, R. Z. Diphenylthiocarbazone immobilized on the triacetyl cellulose membrane as an optical silver sensor. *Turk. J. Chem.* **2008**, *32*, 249–257.

(6) Doyle, F. M.; Liu, Z. D. The effect of triethylenetetraamine (Trien) on the ion flotation of Cu^{2+} and Ni^{2+}. *J. Colloid Interface Sci.* **2003**, *258*, 396–403.

(7) Lazaridis, N. K.; Matis, K. A.; Webb, M. Flotation of metal-loaded clay anion exchangers. Part I: the case of chromate. *Chemosphere* **2001**, *42*, 373–378.

(8) Chen, Q. Y.; Luo, Z.; Hills, C.; Xue, G.; Tyrer, M. Precipitation of heavy metals from wastewater using simulated flue gas: Sequent additions of fly ash, lime and carbon dioxide. *Water Res.* **2009**, *43*, 2605–2614.

(9) Anayurt, R. A.; Sari, A.; Tuzen, M. Equilibrium, thermodynamic and kinetic studies on biosorption of Pb(II) and Cd(II) from aqueous solution by macrofungus (*Lactarius scrobiculatus*) biomass. *Chem. Eng. J.* **2009**, *151*, 255–261.

(10) Donia, A. M.; Atia, A. A.; El-Boraey, H. A.; Mabrouk, D. H. Adsorption of Ag(I) on glycidyl methacrylate/N,N′-methylene bisacrylamide chelating resins with embedded iron oxide. *Sep. Purif. Technol.* **2006**, *48*, 281–287.

(11) Guo, Y.; Din, B.; Liu, Y.; Chang, X.; Meng, S.; Liu, J. Preconcentration and determination of trace elements with 2-aminoacetylthiophenol

functionalized Amberlite XAD-2 by inductively coupled plasma−atomic emission spectrometry. *Talanta* **2004**, *62*, 207–213.

(12) Hruby, M.; Hradil, J.; Benes, M. J. Interactions of phenols with silver(I), copper(II) and iron(III) complexes of chelating methacrylate-based polymeric sorbent containing quinolin-8-ol groups. *React. Funct. Polym.* **2004**, *59*, 105–113.

(13) Atia, A. A.; Donia, A. A.; Yousif, A. M. Comparative study of the recovery of silver(I) from aqueous solutions with different chelating resins derived from glycidyl methacrylate. *J. Appl. Polym. Sci.* **2005**, *97*, 806–812.

(14) Prasad, M.; Saxena, S. Sorption mechanism of some divalent metal ions onto low-cost mineral adsorbent. *Ind. Eng. Chem. Res.* **2004**, *43*, 1512–1522.

(15) Liu, C. K.; Bai, R. B.; Hong, L. Diethylenetriamine-grafted poly(glycidyl methacrylate) adsorbent for effective copper ion adsorption. *J. Colloid Interface Sci.* **2006**, *303*, 99–108.

(16) Li, N.; Bai, R. B. Copper adsorption on chitosan−cellulose hydrogel beads: behaviors and mechanisms. *Sep. Purif. Technol.* **2005**, *42*, 237–247.

(17) Wang, C. R.; Ji, C. N.; Meng, Y. F.; Liu, L.; Qu, R. J.; Wang, C. H. Adsorption Properties of Novel Chelating Resins Containing 2-Amino-5-Methylthio-1,3,4-Thiadizole and Hydrophilic Spacer Arms for Hg^{2+} and Ag. *J. Appl. Polym. Sci.* **2010**, *116*, 636–644.

(18) Chen, Y. Y.; Zhao, Y. Synthesis and characterization of polyacrylonitrile-2-amino-2-thiazoline resin and its sorption behaviors for noble metal ions. *React. Funct. Polym.* **2003**, *55*, 89–98.

(19) Das, D.; Das, A. K.; Sinha, C. A new resin containing benzimidazolylazo group and its use in the separation of heavy metals. *Talanta* **1999**, *48*, 1013–1022.

(20) Pu, Q. S.; Su, Z. X.; Hu, Z. D.; Chang, X. J.; Yang, M. 2-Mercaptobenzothiazole-bonded silica gel as selective adsorbent for preconcentration of gold, platinum and palladium prior to their simultaneous inductively coupled plasma optical emission spectrometric determination. *J. Anal. Atom. Spectrom.* **1998**, *13*, 249–253.

(21) Jeon, C. H.oll, W. H. Chemical modification of chitosan and equilibrium study for mercury ion removal. *Water Res.* **2003**, *37*, 4770–4780.

(22) Alam, T.; Tarannum, H.; Kumar, N.; Kamaluddin Interaction of 2-amino-, 3-amino-, and 4-aminopyridines with chromium and manganese ferrocyanides. *J. Colloid Interface Sci.* **2000**, *224*, 133–139.

(23) Sanchez, J. M.; Hidalgo, M.; Valiente, M.; Salvado, V. New macroporous polymers for the selective adsorption of gold (III) and palladium (II). I. The synthesis, characterization, and effect of spacers on metal adsorption. *J. Polym. Sci. Part A: Polym. Chem.* **2000**, *38*, 269–278.

(24) Qu, R. J.; Sun, C. M.; Ji, C. N.; Wang, C. H.; Zhao, Z. G.; Yu, D. S. Synthesis and adsorption properties of macroporous cross-linked polystyrene that contains an immobilizing 2,5-dimercapto-1,3,4-thiodiazole with tetraethylene glycol spacers. *Polym. Eng. Sci.* **2005**, *45*, 1515–1521.

(25) Sanchez, J. M.; Hidalgo, M.; Salvado, V. The selective adsorption of gold (III) and palladium (II) on new phosphine sulphide-type chelating polymers bearing different spacer arms: Equilibrium and kinetic characterization. *React. Funct. Polym.* **2001**, *46*, 283–291.

(26) Cobianco, S.; Lezzi, A.; Scotti, R. A spectroscopic study of Cu(II)-complexes of chelating resins containing nitrogen and sulfur atoms in the chelating groups. *React. Funct. Polym.* **2000**, *43*, 7–16.

(27) Ji, C. N.; Song, S. H.; Wang, C. R.; Sun, C. M.; Qu, R. J.; Wang, C. H.; Chen, H. Preparation and adsorption properties of chelating resins containing 3-aminopyridine and hydrophilic spacer arm for Hg(II). *Chem. Eng. J.*, **2010**, *165*, 573–580

(28) Denizli, A.; Sanli, N.; Garipcan, B.; Patir, S.; Alsancak, G. Methacryloylamidoglutamic acid incorporated porous poly(methyl methacrylate) beads for heavy-metal removal. *Ind. Eng. Chem. Res.* **2004**, *43*, 6095–6101.

(29) Dong, S. H.; Tang, W. X.; Hu, Y. H. Study on chelating resins XII. Syntheses and adsorption properties of new chelating resins of aminoisopropylmercapto type with a polythioether backbone. *Acta Polym. Sin.* **1990**, *2*, 142–148.

(30) Boyd, G. E.; Adamson, A. W.; Myers, L. S. The exchange adsorption of ions from aqueous solutions by organic zeolites. II. Kinetics. *J. Am. Chem. Soc.* **1947**, *69*, 2836–2848.

(31) Reichenberg, D. Properties of ion-exchange resins in relation to their structure. III. Kinetics of exchange. *J. Am. Chem. Soc.* **1953**, *75*, 589–597.

(32) Saeed, A.; Iqbal, M.; Akhtar, M. W. Removal and recovery of lead(II) from single and multimetal (Cd, Cu, Ni, Zn) solutions by crop milling waste (black gram husk). *J. Hazard. Mater. B* **2005**, *117*, 65–73.

(33) Hameed, B. H.; El-Khaiary, M. I. Sorption kinetics and isotherm studies of a cationic dye using agricultural waste: broad bean peels. *J. Hazard. Mater.* **2008**, *154*, 639–648.

(34) Helfferich, F. *Ion Exchange*; McGraw Hill: New York, 1962; p 166.

(35) Dubinnin, M. M.; Zaverina, E. D.; Radushkevich, L. V. Sorption and structure of active carbon. I. Adsorption of organic vapors. *Zh. Fiz. Khim.* **1947**, *21*, 1351–1362.

(36) Liu, S. H.; Wang, D. H. Pan, C. H. *X-ray electron spectra analysis*; Science Press: Beijing; 1988; p 337.